

Self-gravitating radiation in AdS_d

Vladislav Vaganov

D.A.M.T.P., Centre for Mathematical Sciences, University of Cambridge, Wilberforce Road, Cambridge CB3 0WA, U.K.

E-mail: vv205@cam.ac.uk

ABSTRACT: We study spherically symmetric equilibrium configurations of self-gravitating massless thermal radiation in asymptotically anti-de Sitter space. In $d = 4$, it was shown by Page and Phillips that there is a maximum red-shifted temperature, maximum mass and maximum entropy. For higher central densities, the temperature, mass and entropy undergo an infinite series of damped oscillations, corresponding to unstable configurations. We extend this work to all dimensions $d \geq 3$. We find that in $4 \leq d \leq 10$, the behaviour is similar to the $d = 4$ case. In $d \geq 11$, the temperature, mass and entropy are monotonic functions of the central density, asymptoting to their maxima as the central density goes to infinity. In $d = 3$, an exact solution is given by a slice of the AdS C-metric.

Contents

1. Introduction	1
2. Perfect fluid radiation in asymptotically anti-de Sitter space	3
3. Results	5
4. Comment: validity of perfect fluid approximation	8
5. Conclusions	10
A. Exact solution in $d = 3$	12
B. Phase plane analysis of $\Lambda = 0$ scale-invariant system	15

1. Introduction

It is well known that the canonical ensemble is not defined in asymptotically flat space. This is because having thermal radiation at constant temperature at infinity is not compatible with asymptotic flatness. One can avoid this problem by enclosing the system in a box, which is unphysical [1], or by working in asymptotically anti-de Sitter (*AdS*) space. In *AdS* the canonical ensemble is given by a Euclidean path integral over all matter fields and metrics which tend asymptotically respectively to zero and to *AdS* identified with period $\beta = T^{-1}$ in imaginary time, where T is the red-shifted temperature [1]. In their seminal paper, Hawking and Page [1] studied this path integral in the semiclassical approximation, where it is dominated by classical solutions to the Einstein equations with these boundary conditions. Their work was later generalized to d dimensions [2]. For $T < T_0 = \sqrt{(d-1)(d-3)}/2\pi l$, where $l \gg l_{Planck}$ is the *AdS* length, there are no black hole solutions; thermal radiation, that is, *AdS* periodically identified in imaginary time, is the only admissible phase. For $T_0 < T < T_{HP} = (d-2)/2\pi l$, thermal radiation is the preferred phase, although black holes may form and evaporate from time to time as a result of fluctuations. For $T > T_{HP}$, the configuration with a large *AdS* black hole in equilibrium with thermal radiation has a lower free energy than thermal radiation alone and it therefore dominates the path integral. The point $T = T_{HP}$ marks a first order phase transition, known as the Hawking-Page transition, between two topologically distinct manifolds. The small *AdS* black hole has negative specific heat and is never a dominant phase, but it serves as a bounce mediating the tunneling amplitude between thermal radiation and the large *AdS* black hole [1].

Thus far the gravitational effect of thermal radiation has been neglected, and therefore this picture will undergo quantum corrections when the back-reaction is taken into account. These correspond to the one and higher loop terms in the path integral. An exact solution describing a black hole in equilibrium with thermal radiation remains elusive, although this problem has recently been conjectured to be equivalent to the quest for a localized black hole on a brane [9], which is a purely classical problem in GR. For thermal radiation alone, however, a useful model may be obtained by treating the radiation gas as a perfect fluid with equation of state $p = \rho/(d-1)$, where the energy density is related to the local temperature by the Stefan-Boltzmann law, $\rho \propto T_{loc}^d$. This amounts to taking just the leading term in the high-temperature expansion of the one-loop effective action [10] and is a good approximation if the red-shifted temperature is much greater than the inverse of a characteristic curvature radius of the spacetime. For a given central density, one may solve the Einstein equations with a Λ term for the static spherically symmetric equilibrium configurations of self-gravitating thermal radiation. In $d = 4$, this calculation was carried out by Page and Phillips [3]. Their key finding was that there exist locally stable radiation configurations all the way up to a maximum red-shifted temperature $T_{max} \gg T_{HP}$, above which there are no solutions.¹ Thus for temperatures $T > T_{max}$, the only possible phase is a large *AdS* black hole in equilibrium with thermal radiation [1]. There is also a maximum mass and maximum entropy configuration occurring at a higher central density than the maximum temperature configuration [3]. Beyond their peaks, the temperature, mass and entropy undergo an infinite series of damped oscillations; configurations in this range are unstable, although the precise onset of instability depends on the ensemble [3]. The purpose of this paper is to generalize the analysis of [3] to d dimensions.

The organization is as follows. In section 2 we write down the governing equations for this system, which are a special case of the Tolman-Oppenheimer-Volkoff equations. The solution space is two-dimensional, but if we impose regular boundary conditions at the origin we get a one-parameter set of equilibrium configurations labeled by the central density. These solutions must be found numerically, although useful asymptotic expressions may be obtained when the radius is much smaller or much larger than the *AdS* length. We show how given a solution, one may compute its red-shifted temperature, mass and entropy. We have calculated these for a range of central densities in each dimension. The results are presented in section 3, where we see that in each dimension $d \geq 3$ there is a maximum red-shifted temperature, mass and entropy. However, whereas in $4 \leq d \leq 10$ the behaviour is similar to the $d = 4$ case, in $d \geq 11$ the behaviour is different: the temperature, mass and entropy increase monotonically with the central density, with no oscillations. In section 4 we briefly address the range of validity of the perfect fluid approximation. We conclude in section 5 with a discussion of the broader relevance of this work. Details of the $d = 3$ case are contained in Appendix A. Appendix B contains an analysis of the scale-invariant $\Lambda = 0$ equations.

¹This temperature had previously been estimated in [1]: there it is known as T_2 .

2. Perfect fluid radiation in asymptotically anti-de Sitter space

We want to solve the Einstein equations with radiation gas perfect fluid source for a static spherically symmetric metric in d spacetime dimensions, with asymptotically AdS boundary conditions. We will work in the system of units in which $c = \hbar = k_B = 1$ and $\kappa = 8\pi G_N$. The following is mostly based on [3] extended to d dimensions. The metric may be written as

$$ds^2 = -e^{2\psi} V dt^2 + V^{-1} dr^2 + r^2 d\Omega_{d-2}^2$$

$$V(r) \equiv \left(1 + \frac{r^2}{l^2} - \frac{2\kappa m(r)}{(d-2)\Sigma r^{d-3}} \right), \quad (2.1)$$

where $d\Omega_{d-2}^2$ is the metric on the unit $(d-2)$ -sphere, which has volume Σ . The AdS length $l = (-(d-1)(d-2)/2\Lambda)^{1/2}$, where $\Lambda < 0$ is the cosmological constant. Written in this way,

$$\lim_{r \rightarrow \infty} m(r) = M \quad (2.2)$$

is the total mass of the configuration, and the time coordinate t may be normalized such that

$$\lim_{r \rightarrow \infty} \psi(r) = 0. \quad (2.3)$$

The energy-momentum tensor is taken to be that of a perfect fluid with equation of state $p = \rho/(d-1)$, where p is the isotropic pressure. When the fluid is at rest with respect to the static frame defined by the Killing vector $\partial/\partial t$, this takes the form

$$T_\nu^\mu = \frac{\rho}{d-1} (\delta_\nu^\mu - d\delta_0^\mu \delta_\nu^0), \quad (2.4)$$

where the rest frame energy density is related to the local Tolman temperature T_{loc} through the Stefan-Boltzmann law,

$$\rho = a T_{loc}^d. \quad (2.5)$$

The dimension-dependent constant a is proportional to the effective number of degrees of freedom (see section 4).

The Einstein equations $G_{\mu\nu} + \Lambda g_{\mu\nu} = \kappa T_{\mu\nu}$ for the metric (2.1) and the energy momentum tensor (2.4) yield the following system of ODE's:

$$\frac{dm}{dr} = \Sigma r^{d-2} \rho$$

$$\frac{d\rho}{dr} = -\frac{\rho d [(d-1)(d-3)\kappa m/\Sigma + \kappa r^{d-1} \rho + (d-1)(d-2)r^{d-1}/l^2]}{(d-1)(d-2)r^{d-2}V}, \quad (2.6)$$

which are a case of the Tolman-Oppenheimer-Volkoff equations in d dimensions. There is a two-parameter family of solutions, but imposing regular boundary conditions at the origin,

$$\rho(0) = \rho_c \quad m(0) = 0, \quad (2.7)$$

yields a one-parameter set of regular equilibrium configurations $m(r)$, $\rho(r)$ labeled by the central density $\rho_c > 0$. In general (2.6) must be integrated numerically. Because these

equations are singular at $r = 0$, the solution must be cut off at $r = \epsilon \ll l$, where we set $\rho(\epsilon) = \rho_c$ and $m(\epsilon) = \Sigma \rho_c \epsilon^{d-1} / (d-1)$. The physical answers are recovered as ϵ is taken to zero. In practice, one takes a value of ϵ small enough for the required level of accuracy.²

Once $m(r)$ and $\rho(r)$ (and hence the metric function V) are determined, we turn to the contracted Bianchi identity (equivalently, conservation of $T_{\mu\nu}$), which reads

$$\frac{d\rho}{dr} + \rho d \left(\frac{d\psi}{dr} + \frac{1}{2} V^{-1} \frac{dV}{dr} \right) = 0. \quad (2.8)$$

The red-shifted temperature is defined as

$$T \equiv T_{loc} |g_{tt}|^{1/2} = T_{loc} e^{\psi} V^{1/2}. \quad (2.9)$$

Equation (2.8) implies that T is constant, as it must be for an equilibrium configuration. It follows from condition (2.3) that for large r the solutions behave as $\rho \sim V^{-d/2} \sim r^{-d}$. It also follows that given a solution $m(r)$, $\rho(r)$ the red-shifted temperature may be computed by taking the limit

$$T = \lim_{r \rightarrow \infty} a^{-1/d} \rho^{1/d} V^{1/2}. \quad (2.10)$$

Equation (2.9) may then be used to determine $\psi(r)$. Note that for the regular solutions we are considering, equations (2.6) and (2.8) imply $dm/dr > 0$, $d\rho/dr < 0$ and $d\psi/dr > 0$ for all $r > 0$. Pure *AdS* in global coordinates corresponds to $\rho_c = 0$ and has $m = \rho = \psi = 0$ for all $r \geq 0$.

One may compute the entropy S of an equilibrium configuration by integrating the local entropy density,

$$s = \frac{d}{d-1} a T_{loc}^{d-1} = \frac{d}{d-1} a^{1/d} \rho^{(d-1)/d} \quad (2.11)$$

over the proper spatial volume:

$$S = \frac{d}{d-1} a^{1/d} \Sigma \int_0^\infty \rho^{(d-1)/d} V^{-1/2} r^{d-2} dr. \quad (2.12)$$

If the mass (2.2) and temperature (2.10) are known for a range of central densities, the entropy may also be obtained by integrating the first law of thermodynamics, $dM = T dS$, starting from the $\rho_c = 0$ configuration which has $M = T = S = 0$.

We now go on to consider certain limits of the solutions. Observe that equations (2.6) are invariant [5] under the scaling

$$r \rightarrow Cr, \quad \rho \rightarrow C^{-2} \rho, \quad m \rightarrow C^{d-3} m, \quad l \rightarrow Cl, \quad (2.13)$$

where $C \in \mathbb{R}^+$. When $\Lambda = 0$ ($l = \infty$) this is an exact scale invariance [6]. In this case there exists a special self-similar solution³ given by

$$\rho = \alpha r^{-2}, \quad m = \alpha \Sigma r^{d-3} / (d-3) \quad \text{where} \quad \alpha = \frac{2(d-1)(d-3)\kappa^{-1}}{d^2 - d + 2}, \quad (2.14)$$

²It is possible to regularize the Tolman-Oppenheimer-Volkoff equations and recast them as a 3-dimensional regular dynamical system on a compact state space [19]. This has a number of advantages, but is not essential in our analysis, see, however, Appendix B.

³By this we mean the self-similarity of the geometry as captured by the existence of a proper homothetic vector [7]. This does not necessarily follow from the self-similarity of the matter fields as expressed by the scaling relation (2.13) with $\Lambda = 0$. Indeed, other solutions of the $\Lambda = 0$ equations do not admit a proper homothetic vector.

and we take $d \geq 4$ (see Appendix A for the $d = 3$ case). This solution is singular at $r = 0$. It is the limit as the central density goes to infinity of the $\Lambda = 0$ solutions with a regular origin. The latter may be computed numerically, see, for example, [4, 17] for $d = 4$. It is best formulated (Appendix B) using variables invariant under the scale transformation (2.13), whence equations (2.6) may be reduced to a plane autonomous system, from which one may derive various qualitative features and asymptotic approximations [4, 17]. For large r , regular solutions will approach the self-similar solution (2.14), which has infinite mass and is thus not asymptotically flat. To obtain finite mass solutions in the $\Lambda = 0$ case, one must confine the radiation to an unphysical box. If one does so, the thermodynamics (red-shifted temperature, mass and entropy as functions of the central density) of these configurations will be qualitatively similar to the asymptotically *AdS* case studied here.

For fixed $\Lambda < 0$, equations (2.6) are no longer scale invariant. However, for $r \ll l$, the terms involving Λ may be neglected, and the solutions approach the regular $\Lambda = 0$ solution with the same value of ρ_c . In the limit as the central density goes to infinity, they approach the singular self-similar solution (2.14) for $r \ll l$. On the other hand, for large r , $\rho \sim r^{-d}$, and the first of equations (2.6) implies that the mass of these solutions is finite. This is due to the confining nature of the gravitational potential in anti-de Sitter space, which acts as a box of finite volume.

3. Results

For each dimension, we computed a number of solutions for a range of values of ρ_c , and the red-shifted temperature, mass and entropy for each solution. A combination of Runge-Kutta methods were used to integrate equations (2.6) starting from $r = \epsilon$ and terminating at $r = r_1 \gg l$, and then equations (2.10), (2.2) and (2.12) with infinity replaced by r_1 were used to evaluate the temperature, mass and entropy. The configuration with infinite central density was computed by imposing (2.14) as a boundary condition at $r = \epsilon$. The errors coming from neglecting the region $r_1 < r < \infty$ may be approximated by using asymptotic expansions [3]. The accuracy of the calculation depends on the values of ϵ , r_1 and the error tolerance of the routine. A range of different values were used to achieve four-significant-figure accuracy, where greater precision was required at higher central densities and in higher dimensions. We work in terms of the dimensionless quantities

$$\begin{aligned}\tilde{\rho}_c &\equiv \kappa l^2 \rho_c \\ \tilde{T} &\equiv a^{1/d} \kappa^{1/d} l^{2/d} T \\ \tilde{M} &\equiv \kappa l^{3-d} M \\ \tilde{S} &\equiv a^{-1/d} \kappa^{(d-1)/d} l^{-(d-1)(d-2)/d} S.\end{aligned}\tag{3.1}$$

We found that for all $d \geq 3$ there exists a maximum red-shifted temperature, T_{max} , a maximum mass M_{max} and a maximum entropy S_{max} , where the maximum entropy configuration always coincides with the maximum mass configuration. The maxima of temperature, mass and entropy, along with the corresponding values of ρ_c , are presented in Table 1 for $3 \leq d \leq 13$. For comparison, we also give the ratio of \tilde{M}_{max} to the mass $\tilde{M}_{HP} = (d-2)\Sigma$

of the large AdS black hole at the Hawking-Page temperature: this is simply to illustrate the similar dimensional dependence of these quantities (see section 4 for some physical comparisons). Figs. 1-3 show how the dimensionless temperature, mass and entropy vary with the central density for three representative cases: $d = 4$, $d = 11$ and $d = 3$.

d	$\ln \tilde{\rho}_c$	\tilde{T}_{max}	$\ln \tilde{\rho}_c$	\tilde{M}_{max}	$\tilde{M}_{max}/\tilde{M}_{HP}$	\tilde{S}_{max}
3	0	$2/3 \approx 0.6667$	$\ln 4 \approx 1.386$	$\pi/3 \approx 1.047$	$1/3 \approx 0.3333$	$4^{2/3}\pi \approx 7.916$
4	1.353	0.9479	2.018	11.56	0.4598	15.22
5	2.349	1.081	2.650	22.98	0.3880	25.95
6	3.234	1.145	3.354	37.76	0.3586	39.22
7	4.119	1.177	4.158	53.39	0.3444	52.78
8	5.109	1.190	5.119	66.55	0.3354	63.81
9	6.390	1.195	6.392	74.50	0.3278	70.08
10	8.590	1.195	8.590	76.08	0.3204	70.72
11	∞	1.192	∞	71.81	0.3129	66.25
12	∞	1.188	∞	63.31	0.3055	58.14
13	∞	1.183	∞	52.57	0.2983	48.15

Table 1: Maximum red-shifted temperature, maximum mass and maximum entropy configurations of spherically symmetric thermal radiation in AdS in various dimensions. The quantity $\tilde{M}_{HP} = (d - 2)\Sigma$ is the mass of the large AdS black hole at the Hawking-Page temperature.

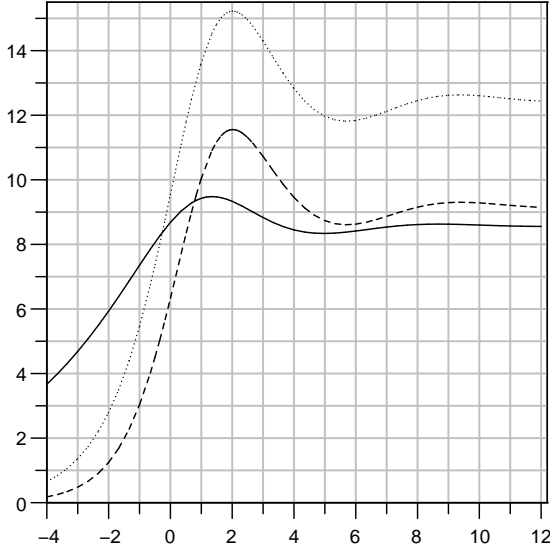


Figure 1: $d = 4$: $10\tilde{T}$ (solid line), \tilde{M} (dashed line) and \tilde{S} (dotted line) vs. $\ln \tilde{\rho}_c$

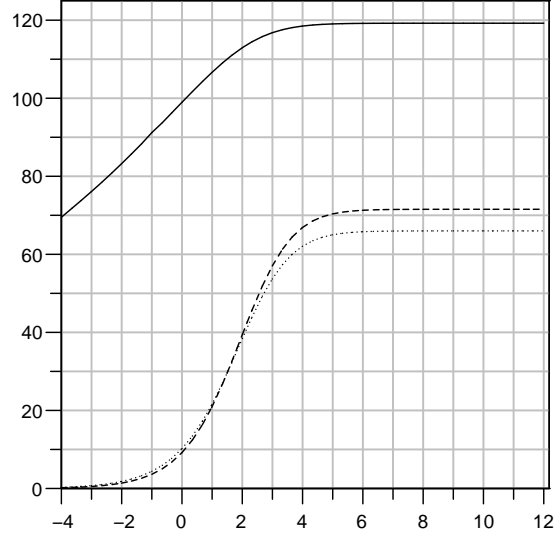


Figure 2: $d = 11$: $10^2\tilde{T}$ (solid line), \tilde{M} (dashed line) and \tilde{S} (dotted line) vs. $\ln \tilde{\rho}_c$

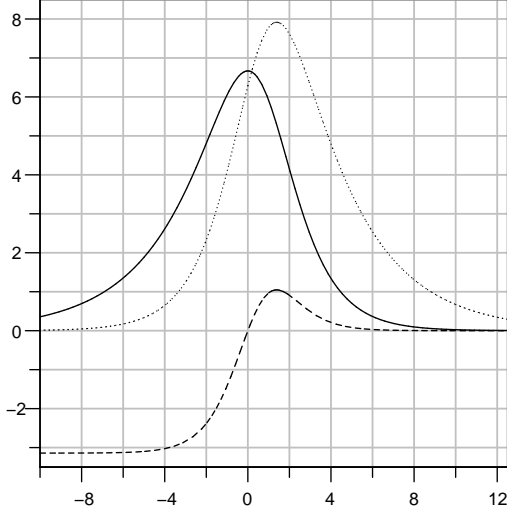


Figure 3: $d = 3$: $10\tilde{T}$ (solid line), \tilde{M} (dashed line) and \tilde{S} (dotted line) vs. $\ln \tilde{\rho}_c$

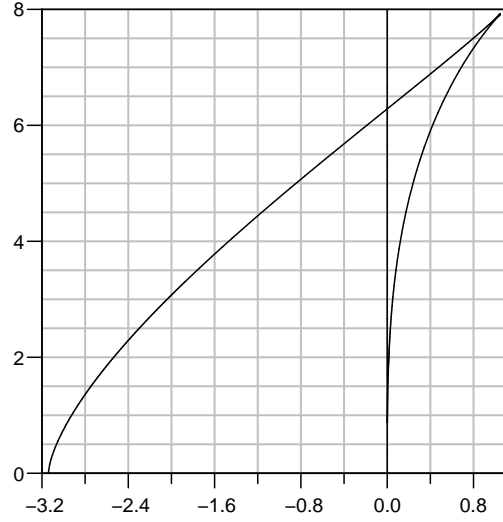


Figure 4: $d = 3$: \tilde{S} (ordinate) vs \tilde{M} (abscissa)

Our main findings are summarized below:

- $4 \leq d \leq 10$. The behaviour is similar to the $d = 4$ case which is illustrated in Fig. 1. To the right of their respective peaks, the temperature, mass and entropy exhibit an infinite series of damped oscillations: configurations in this range are unstable to one or more radial modes, although the precise onset of instability depends on the ensemble [3]. In the canonical ensemble, at fixed red-shifted temperature, all configurations to the right of T_{max} are unstable. In the microcanonical ensemble, at fixed mass, all configurations to the right of M_{max} are unstable. The maximum temperature configuration always occurs at a lower central density than the maximum mass and entropy configuration (note that for $d = 10$ they lie very close). The numerical values given in Table 1 for $d = 4$ agree with [3].
- $d \geq 11$. In this case the red-shifted temperature, mass and entropy increase monotonically with the central density, asymptoting to their maximum values as the central density goes to infinity, see Fig. 2. Since the specific heat is always positive, one would expect these configurations to be stable for all values of ρ_c . To the author's knowledge, this case has not been studied before. Note that this critical dimension was found analytically and not numerically: its exact (non-integer) value is in fact just under 11, see Appendix B.

- **d = 3.** In this special case an exact solution exists, see Appendix A. We found the following expressions for the (dimensionless) red-shifted temperature, mass and entropy:

$$\tilde{T} = \frac{\tilde{\rho}_c^{1/3}}{1 + \tilde{\rho}_c/2} \quad (3.2)$$

$$\tilde{M} = \frac{\pi(\tilde{\rho}_c - 1)}{(1 + \tilde{\rho}_c/2)^2} \quad (3.3)$$

$$\tilde{S} = \frac{3\pi\tilde{\rho}_c^{2/3}}{1 + \tilde{\rho}_c/2}. \quad (3.4)$$

These are plotted in Figs. 3 and 4. Here the mass is defined such that it vanishes for the massless BTZ black hole. The minimum mass $M = -1/8G_3$ ($\tilde{M} = -\pi$) corresponds to AdS_3 in global coordinates. The maximum mass is $M = 1/24G_3$ ($\tilde{M} = \pi/3$). This is the same as the range of masses found for black holes localized on an AdS_3 brane [8].⁴ The limiting infinite central density solution is the same as the massless BTZ black hole except that there is a curvature singularity proportional to a δ -distribution supported at the origin (Appendix A). As in the $4 \leq d \leq 10$ case, one would expect that configurations to the right of the peak of temperature (mass) in Fig. 3 are unstable to radial perturbations with canonical (microcanonical) boundary conditions.

4. Comment: validity of perfect fluid approximation

Under what conditions is this a good model of quantum fluctuations about the thermal AdS saddle point (that is, AdS periodically identified in imaginary time)? For a general (non-conformal, self-interacting, arbitrary spin) field theory in a static curved spacetime, the energy-momentum tensor (2.4) with the Stefan-Boltzmann relation (2.5) corresponds to the leading term in the high-temperature expansion of the one-loop effective action [10, 11, 12]. The higher order terms will be small if the red-shifted temperature satisfies $T \gg \mathcal{R}^{-1}$ and $T \gg m_{eff}$, where \mathcal{R} is a characteristic curvature radius of the spacetime and m_{eff} is the effective mass of the field [11].⁵ The constant a is proportional to the effective number of massless degrees of freedom g :

$$a = (d-1)\pi^{-d/2}\Gamma\left(\frac{d}{2}\right)\zeta(d)g, \quad \text{where} \quad g = n_B + \left(1 - 2^{-(d-1)}\right)n_F, \quad (4.1)$$

with n_B being the number of boson spin states and n_F the number of fermion spin states. This may be obtained by integrating the d -dimensional Planck distribution over all frequencies, taking into account the degeneracy of states factor, see, for example, [13]. Note that we are also assuming that the characteristic curvature radius \mathcal{R} is much greater than

⁴Fig. 4 should be compared to Fig. 1 in [8] although the dependence of the entropy and temperature on the other parameters (G_3 , l , a) is different for the two cases. The expressions for the mass, temperature and entropy in [8] also depend on the parameter λ , which is related to the positions of the two branes.

⁵In general, the effective mass will contain a term involving the Ricci scalar, as well as terms involving the interaction potential. However, since we are expanding about the trivial $\Psi = 0$ background, there will not be any interaction terms.

the Planck length l_{Planck} so that vacuum polarization terms and higher order quantum gravity effects are negligible.

In the context of the configurations studied in this paper, we can be more precise. If the field is massless (or if the red-shifted temperature is well above the rest mass), the condition for the higher order terms in the high-temperature expansion to be small becomes

$$T \gg \max\{(\kappa\rho_c)^{1/2}, l^{-1}\}, \quad (4.2)$$

since for $\kappa\rho_c \gtrsim l^{-2}$ the origin will be the place of maximum curvature. Now $d\psi/dr > 0$ and condition (2.3) imply $\psi(0) < 0$. From equation (2.9) and $V(0) = 0$ it follows that $T_{loc}(0) > T$. Equation (4.2) and the Stefan-Boltzmann relation (2.5) may then be used to show that the higher order terms are small if the dimensionless temperature satisfies

$$\gamma^{-1/d} \ll \tilde{T} \leq \tilde{T}_{max}, \quad (4.3)$$

or if the dimensionless density falls in the range

$$\gamma^{-1} \ll \tilde{\rho}_c \ll \gamma^{2/d}, \quad (4.4)$$

where $\gamma \equiv a^{-1}(l/l_{Planck})^{d-2}$. For $l \gg l_{Planck}$, as we have assumed, and if the number of degrees of freedom is not too large, γ is a large number and this model is applicable in a wide domain.⁶ In that case, in $3 \leq d \leq 10$, the majority of the configurations corresponding to the curves in Fig. 1 and Fig. 3 would belong to this regime, including the maximum temperature configuration. On the other hand, in $d \geq 11$ (Fig. 2), the maximum temperature configuration corresponds to infinite central density and therefore higher order terms would come into play well before this point is reached. It would be interesting to understand better the significance of this.

The same factor γ appears if we compare the maximum temperature of thermal radiation to the Hawking-Page temperature $T_{HP} = (d-2)/2\pi l$: we find $T_{max}/T_{HP} \sim \gamma^{1/d} \gg 1$ if $\gamma \gg 1$. This is consistent, since thermal radiation heated to a temperature $T > T_{max}$ must collapse to a black hole with a lower free energy. Similarly, if we follow [1] and consider the microcanonical ensemble at fixed energy E , it may be estimated that an equilibrium of a black hole with thermal radiation is more probable than thermal radiation alone if $E > E_1$, where

$$E_1^{2d-3} \sim \kappa^{-d} a^{d-3} l^{(d-1)(d-3)}. \quad (4.5)$$

For consistency we require $M_{max} > E_1$ and indeed we find $M_{max}/E_1 \sim \gamma^{(d-3)/(2d-3)} \gg 1$, assuming $d > 3$.⁷ Furthermore, we may compare the maximum entropy of thermal radiation to the entropy of a black hole of the same mass, $S_{BH} = 2\pi\Sigma\kappa^{-1}r_H^{d-2}$, where r_H is the horizon radius: we find $S_{max}/S_{BH} \sim \gamma^{-1/d} \ll 1$, which is consistent with the Bekenstein bound. Note that these comparisons should not be taken too literally, since we should really be comparing the radiation values to the black hole values calculated at the one-loop level.

⁶The upper limits in (4.3) and (4.4) are well below the Planck scale in that case.

⁷In $d = 3$, there exists a stable equilibrium of a BTZ black hole and thermal radiation for any $E > 0$.

5. Conclusions

We have studied spherically symmetric equilibria of perfect fluid radiation with asymptotically AdS boundary conditions in various dimensions. As in the $d = 4$ case, there is a maximum red-shifted temperature, maximum mass and maximum entropy in all dimensions $d \geq 3$. We computed these values for $3 \leq d \leq 13$. In $d = 3$ the analytical results serve as a useful toy model, although it must be kept in mind that $2 + 1$ gravity has some special properties that do not necessarily carry over into higher dimensions. In $4 \leq d \leq 10$ the behaviour is similar to the $d = 4$ case studied in [3]. In $d \geq 11$ there is a qualitative difference in behaviour: the temperature, mass and entropy are monotonic functions of the central density, approaching their maximum values as the central density tends to infinity, with no oscillations. Whilst we are not certain of the significance of the latter result, what we can say is that it applies in a more general setting than that of a radiation fluid. The oscillatory profile of thermodynamic variables at high central densities, associated with modes of instability, is a feature of a wide class of stellar models: it appears in general relativity whenever the high density core of a star is described by a gamma-law equation of state [14, 17, 19], or indeed certain polytropic equations of state [15], as well as in Newtonian theory (the isothermal sphere [16]), and is independent of the properties of the outer regions [19]. As shown in the dynamical systems analysis of [19], for an asymptotically gamma-law equation of state, it can be traced to the nature of the self-similar solution (2.14), which is a fixed point of the Tolman-Oppenheimer-Volkoff equations. In $d = 4$ it is a stable focus, resulting in oscillatory behaviour in the high density limit. Their analysis may be extended to d dimensions, see Appendix B. We found that in $4 \leq d \leq 10$ it is a stable focus, whereas in $d \geq 11$ it is a stable node, resulting in monotonic profiles, as seen in this paper.

One may also look at these solutions from another perspective, which comes from considering the connection between dynamics and thermodynamics [4]. The entropy of a given state is expected to measure the logarithm of the fraction of time the system spends in that state throughout its dynamical history [20]. For matter configurations, this has the implication that the stable equilibrium configurations should correspond to local maxima of the entropy at fixed energy [4]. The relevance of this is as follows. Firstly, it may be shown that all static spherically symmetric asymptotically AdS configurations of a radiation fluid, i.e. the solutions to the Tolman-Oppenheimer-Volkoff equations (2.6) are extrema of the total entropy (2.12).⁸ The converse statement, that the solutions to equations (2.6) are the only extrema of the entropy, would hold only if it can be assumed that all extrema are spherically symmetric and that all fluid spacetimes of the type considered contain a maximal hypersurface [4]. Existence of maximal hypersurfaces in asymptotically flat [21] and asymptotically AdS [22] spacetimes has been proved subject to certain conditions. The long-standing conjecture that a static perfect fluid star in $d = 4$ is necessarily spherically symmetric appears to have been proved in [23] for physically reasonable equations of state in asymptotically flat space. It is not known if a result of this kind exists in asymptoti-

⁸This was shown in [4] for the $\Lambda = 0$, $d = 4$ case of radiation in a box of fixed radius, but it extends to the asymptotically AdS case.

cally AdS space, in arbitrary dimension. Note that in the asymptotically AdS case one can consider more general conformal structures at infinity, the so-called asymptotically locally AdS spacetimes [24]. Thus in this paper we only dealt with a restricted class of solutions. Secondly, [4] showed that in the $\Lambda = 0$, $d = 4$ case of radiation in a box, the criterion for thermodynamic stability – that the extremum is a strict local maximum of the entropy – is equivalent to the condition for dynamical stability under linear radial perturbations. This stability argument would be expected to generalize to the asymptotically AdS case in d dimensions, although it would be useful to carry out a detailed perturbation analysis. A similar formulation should also be possible in the canonical ensemble, where stable equilibria should correspond to local minima of the free energy at fixed red-shifted temperature.

Finally, it would be interesting to consider these solutions in the context of the Karch-Randall model, where one has an asymptotically AdS_{d-1} brane in an AdS_d bulk [25, 26]. According to AdS/CFT , classical dynamics in the bulk is dual to the quantum dynamics of a CFT living on the brane, in the planar limit, coupled to $(d-1)$ -dimensional Einstein gravity. The strongly-coupled CFT has a UV cutoff $\sim 1/L$ and an IR cutoff $\sim 1/l$, where L and l are respectively the bulk and brane AdS lengths. This theory has been interpreted as a defect CFT [27], although there are a number of issues still to be resolved. In the original Karch-Randall model, the bulk volume is infinite and the zero mode graviton is not normalizable, nevertheless for $l \gg L$ there is an ultralight graviton with a tiny mass $m^2 \sim L^{d-3}/l^{d-1}$ and $(d-1)$ -dimensional gravity is effectively reproduced at distances $r \gtrsim L$ on the brane, although its mass, and the extra dimension, would become apparent at very large distances $r \gtrsim l^{d-2}/L^{d-3}$ [26].⁹ However, if one introduces into the bulk a second positive tension AdS_{d-1} brane [28, 29], one recovers the zero mode and $(d-1)$ dimensional gravity is valid all the way to infinity. One now has two gravitons: the massless one and the ultralight one, although the ultralight one decouples in the limit that the second brane approaches the turn-around point of the warp factor [29]. Now if the metric on one of the branes is given exactly by one of the thermal radiation configurations studied in this paper, one may wonder what happens in the bulk? In this context, it is interesting to note that in the $d = 4$ version of this model, with two AdS_3 branes in an AdS_4 bulk, the bulk metric is the AdS C-metric studied in [8] and the other brane contains a localized black hole (Appendix A). It would be interesting to see if this property is just a special feature of this lower dimensional model or whether there is a regime where it would hold in higher dimensions. We note that the issue of the Hawking-Page transition in this setup has been addressed in [30], although only in the limit $l/L \rightarrow \infty$ where matter effects can be ignored.

Note

After this work first appeared, two other papers came out, one by John Hammersley [40] and one by Pierre-Henri Chavanis [41], who have been independently working on similar problems. Specifically, [40] studies self-gravitating radiation in d -dimensional AdS and also

⁹For $L \lesssim r \lesssim l$ the $(d-1)$ -dimensional graviton is a composite made out of the ultralight mode and heavier Kaluza-Klein modes, whereas for $l \lesssim r \lesssim l^{d-2}/L^{d-3}$ it is just the ultralight mode [26].

finds the change in behaviour from oscillatory in $4 \leq d \leq 10$ to monotonic in $d \geq 11$ (note that the $d = 5$ case had previously appeared in [39] in a study of bulk-cone singularities in *AdS/CFT*). He points out the possibility that (besides a possible link to string theory!) this could be related to a similar dimensional transition found in a cosmological setting [37, 38], where the analysis of Belinsky, Khalatnikov and Lifshitz (BKL) [36] was extended to arbitrary dimension, with the finding that the chaotic oscillatory dynamics of the gravitational field close to a spacelike singularity for $4 \leq d \leq 10$ is replaced by a monotonic power law time dependence for $d \geq 11$. It would be interesting to explore this connection further.

The work of [41] is a comprehensive study of the behaviour of general relativistic perfect fluid stars with a linear equation of state in d dimensional asymptotically flat space (in a box), including the radiation case, extending the analysis of [17] to arbitrary dimension (the Newtonian case had previously been treated in [35]). He also finds that for $d \geq 11$ the oscillatory behaviour disappears. In fact the results of Sec. 6.4 in [41] are consistent with the findings noted in Appendix B of this paper and provide an alternative derivation of the asymptotic behaviour of $\Lambda = 0$ linear perfect fluid solutions in different dimensions. The paper [41] also includes a detailed stability analysis of the different regimes, with the suggestion that for these solutions thermodynamic stability is equivalent to *nonlinear* dynamical stability. The $d = 3$ case, treated in Appendix A of this paper, is also analyzed, although the author suggests that these solutions have finite radial extent whereas, as noted in Appendix A, the finite radial coordinate at which the density vanishes is at infinite proper distance from any other point in the spacetime.

Acknowledgments

The author would like to thank Stephen Hawking for many helpful discussions and advice. The author would also like to thank Claes Uggla for useful correspondence on self-similarity and James Lucietti and Gian Paolo Procopio for comments on this manuscript.

A. Exact solution in $d = 3$

In this appendix we derive exact solutions for regular equilibrium configurations of thermal radiation in $d = 3$, both for $\Lambda < 0$, and for $\Lambda = 0$. Garcia and Campuzano [31] have obtained all static circularly symmetric perfect fluid solutions in $2 + 1$ dimensions, and the solutions below belong to one of the classes presented in that paper. We found it interesting, however, that the case of a radiation fluid with $\Lambda < 0$ may also be obtained starting from the *AdS* C-metric studied by Emparan, Horowitz and Myers [8], describing black holes accelerating in *AdS*₄. This metric, which is a static axially symmetric vacuum solution to the four-dimensional Einstein equations with negative cosmological constant, takes the form

$$ds^2 = \frac{1}{A^2(x-y)^2} \left[H(y)dt^2 - \frac{dy^2}{H(y)} + \frac{dx^2}{G(x)} + G(x)d\phi^2 \right], \quad (\text{A.1})$$

where

$$\begin{aligned} H(y) &= -\lambda + ky^2 - 2\mu Ay^3 \\ G(x) &= 1 + kx^2 - 2\mu Ax^3, \end{aligned} \quad (\text{A.2})$$

with $\lambda > 0$, $A > 0$, $\mu > 0$ and $k = -1, 0, +1$. Points with $x = y$ correspond to the boundary of the asymptotically AdS_4 geometry, therefore the solution is restricted to the region $y < x$. The coordinate ϕ is an angle and each zero of $G(x)$ corresponds to an axis for the rotation symmetry, where we need $G(x) \geq 0$ to preserve the Lorentzian signature. For $\mu > 0$, $G(x)$ has only one positive root x_2 and in order to avoid a conical singularity at this point, the periodicity of the angular coordinate ϕ is set to be $\Delta\phi = 4\pi/|G'(x_2)|$. The smallest zero of $H(y)$ defines the black hole horizon. See [8] for further details. The authors of [8] considered putting two positive tension asymptotically AdS_3 branes in this spacetime: one at $x = 0$, the black hole brane, and a second non-singular brane at $y = 0$. This is a lower dimensional version of the two-brane Karch-Randall model where, at least in a certain range of parameter space, bulk gravity in AdS_4 is expected to reproduce AdS_3 gravity on each brane, plus quantum corrections coming from a CFT. The different values of k correspond to different slicings of AdS_3 .¹⁰ Now, if there is a quantum corrected black hole on the first brane, then the other non-singular brane at $y = 0$ should correspond to thermal radiation in AdS_3 at constant red-shifted temperature. This may verified by examining the induced metric on the surface $y = 0$,

$$ds^2 = \frac{1}{A^2 x^2} \left[-\lambda dt^2 + \frac{dx^2}{G(x)} + G(x) d\phi^2 \right], \quad (\text{A.3})$$

where x is restricted to lie in the range $0 < x \leq x_2$. The Einstein tensor for this 3-metric is

$$G_\nu^\mu = A^2 \text{diag}(1, 1, 1) + \mu A^3 x^3 \text{diag}(-2, 1, 1), \quad (\text{A.4})$$

which describes a $p = \rho/2$ perfect fluid with density

$$\rho = \frac{2\mu A^3 x^3}{8\pi G_3} \quad (\text{A.5})$$

in a spacetime with cosmological constant $\Lambda = -1/l^2 = -A^2$. To convert this to the standard BTZ form, that is

$$ds^2 = -N^2 dt^2 + \left(\frac{r^2}{l^2} - 8G_3 m \right)^{-1} dr^2 + r^2 d\theta^2, \quad 0 \leq \theta \leq 2\pi, \quad (\text{A.6})$$

where $N(r)$ is the lapse function, change variables to the following:

$$\begin{aligned} r &= \frac{2}{A|G'(x_2)|} \frac{\sqrt{G(x)}}{x}, \\ \theta &= \frac{|G'(x_2)|}{2} \phi. \end{aligned} \quad (\text{A.7})$$

¹⁰In the $\mu = 0$ case when the bulk metric (A.1) is locally AdS_4 , $k = -1$ corresponds to global coordinates on the AdS_3 slices, whilst $k = 0$ and $k = 1$ give the metrics of the massless and massive BTZ black holes respectively [8].

Observe that $x = x_2$ corresponds to $r = 0$, and $x = 0$ corresponds to $r = \infty$. It is not possible to express the functions m , ρ and N in a simple form in terms of r , nevertheless, it is possible to obtain explicit expressions for the red-shifted temperature, mass and entropy. In terms of the dimensionless variables (3.1), we find

$$\begin{aligned}\tilde{T} &= \frac{\tilde{\rho}_c^{1/3}}{1 + \tilde{\rho}_c/2} \\ \tilde{M} &= \frac{\pi(\tilde{\rho}_c - 1)}{(1 + \tilde{\rho}_c/2)^2} \\ \tilde{S} &= \frac{3\pi\tilde{\rho}_c^{2/3}}{1 + \tilde{\rho}_c/2}.\end{aligned}$$

Note that in the metric (A.3), the different values $k = -1$, $k = 0$ and $k = 1$ are mapped to the ranges $0 \leq \tilde{\rho}_c < 1$, $\tilde{\rho}_c = 1$ and $\tilde{\rho}_c > 1$ respectively. Consider now the limit $\rho_c \rightarrow \infty$. Equations (A.2) and (A.5) require $\mu A \rightarrow 0$ and $x_2 \approx (2\mu A)^{-1} \rightarrow \infty$. The limiting solution has $\rho = 0$ and $m = 0$ for all $r > 0$ which is the same as the massless BTZ black hole. However, there is a curvature singularity proportional to a δ -distribution supported at the origin.

The $\Lambda = 0$ case may be obtained from the metric (A.3) by making the transformation $\hat{x} = Ax$, $\hat{\phi} = A^{-1}\phi$, $\hat{G} = A^2G$ and taking the limit $A \rightarrow 0$. Dropping the hats, this gives the 3-metric

$$ds^2 = \frac{1}{x^2} \left[-\lambda dt^2 + \frac{dx^2}{G(x)} + G(x) d\phi^2 \right], \quad (\text{A.8})$$

where $G(x) = kx^2 - 2\mu x^3$ and the period of ϕ is $4\pi/|G'(x_2)|$. The Einstein tensor for this metric is

$$G^\mu_\nu = \mu x^3 \text{diag}(-2, 1, 1), \quad (\text{A.9})$$

which describes a $p = \rho/2$ perfect fluid with density

$$\rho = \frac{2\mu x^3}{8\pi G_3}. \quad (\text{A.10})$$

and $\Lambda = 0$. Making the choice $k = 1$ (this is the only consistent choice), we restrict to $0 < x \leq x_2 = 1/2\mu$ so that $G(x) \geq 0$. We may compare the metric (A.8) to a more standard form for $\Lambda = 0$ static solutions in 2 + 1 gravity:

$$ds^2 = -N^2 dt^2 + (1 - 4G_3 m)^{-2} dr^2 + r^2 d\theta^2, \quad 0 \leq \theta < 2\pi, \quad (\text{A.11})$$

where $N(r)$ is the lapse function.¹¹ Now in three dimensions the Weyl tensor vanishes so the spacetime outside a point mass is locally flat [32]: the point mass only affects the spacetime globally, making it into a cone, the value of the mass being given by the conical deficit angle at infinity, $\delta_\infty = 8\pi G_3 m$. Note that this differs from the mass defined by the metric (A.6) with $\Lambda = 0$. In particular $m = 1/4G_3$ in the normalization of (A.11) corresponds to $m = 0$ in the $\Lambda = 0$ version of (A.6). Note also that in the case under consideration, we

¹¹This differs from the usual form [32, 33] by a trivial change of variables.

are dealing not with point sources but with smooth perfect fluid configurations. Changing variables to

$$\begin{aligned} r &= \frac{2}{|G'(x_2)|} \frac{\sqrt{G(x)}}{x} = 4\mu\sqrt{1-2\mu x}, \\ \theta &= \frac{|G'(x_2)|}{2} \phi = \frac{\phi}{4\mu}, \end{aligned} \tag{A.12}$$

we see that $x = x_2$ corresponds to $r = 0$, and $x = 0$ corresponds to $r = r_{max} = 4\mu > 0$. The radial coordinate is bounded: $0 \leq r < r_{max}$. After some algebra we obtain the following expressions for the mass, density and lapse function of the regular radiation fluid configurations with $\Lambda = 0$:

$$\begin{aligned} m &= \frac{1}{4G_3} \left[1 - (1 - 2\pi G_3 \rho_c r^2)^2 \right] \\ \rho &= \rho_c (1 - 2\pi G_3 \rho_c r^2)^3 \\ N &= N_0 (1 - 2\pi G_3 \rho_c r^2)^{-1}, \end{aligned} \tag{A.13}$$

where $\rho_c = (32\pi G_3 \mu^2)^{-1}$ is the central density. The mass varies from $m = 0$ at $r = 0$ to $m \rightarrow 1/4G_3$ as the radius $r \rightarrow r_{max}$. This is exactly the range of masses one would expect in $2+1$ gravity with zero cosmological constant with smooth matter sources [33]. It may be verified that the proper distance between two points in the spacetime diverges if the radial coordinate of one of them approaches r_{max} : thus $r = r_{max}$ lies at infinity and the solutions are unbounded. There are no conical singularities: the conical deficit angle increases smoothly from zero at $r = 0$ and tends to 2π as $r \rightarrow r_{max}$. One may visualize the geometry represented by the the spatial part of the metric (A.11) by embedding it into a 3-dimensional flat Euclidean space (r, θ, z) : one ends up with a semi-infinite cigar, asymptoting to a cylinder at infinity.¹² The cylinder is the $d = 3$ analogue of the singular self-similar solution (2.14): it is the geometry of a point particle at the origin of mass $M = 1/4G_3$ (in particular, $\rho = 0$ for all $r > 0$) [32]. As in the $d > 3$ case, this solution also corresponds to the $\rho_c \rightarrow \infty$ limit of the $\Lambda < 0$ radiation fluid configurations for $r/l \rightarrow 0$. In that case, the second of equations (2.6) implies that $\rho = 0$ for all $r > 0$. This explains our previous observation, that the $\rho_c \rightarrow \infty$ limit of the $\Lambda < 0$ radiation fluid configurations is the same as a massless BTZ black hole for $r > 0$.

B. Phase plane analysis of $\Lambda = 0$ scale-invariant system

In this appendix we outline a dynamical systems analysis of the d -dimensional Tolman-Oppenheimer-Volkoff equations in the $\Lambda = 0$ case, which yields an exact (non-integer) value for the critical dimension at which the oscillatory behaviour ceases. For generality, we assume a linear (“gamma-law”) equation of state $p = q\rho$, with $0 \leq q \leq 1$: this leads to

¹²As noted in [41], these unbounded solutions are marginally stable (as in the $d \geq 4$ case). However, one may enclose the fluid in a box of finite proper radius and match it on the outside to a cone to obtain stable asymptotically conical solutions.

the equations being scale invariant, which greatly facilitates the analysis. We also restrict attention to $d \geq 4$ (the $d = 3$ case must be treated separately, we do not describe it here). In $d = 4$, analogous phase portraits have been considered in [4, 6, 17] using non-compact variables. We follow the formulation introduced in [19], in which the state space of the dynamical system is compact, i.e. the boundaries are included.

The Tolman-Oppenheimer-Volkoff equations in d dimensions with $\Lambda = 0$ read:

$$\begin{aligned} \frac{dm}{dr} &= \Sigma r^{d-2} \rho \\ \frac{dp}{dr} &= -\frac{(d-3)\kappa m \rho}{(d-2)\Sigma r^{d-2}} \left(1 + \frac{p}{\rho}\right) \left(1 + \frac{\Sigma r^{d-1} p}{(d-3)m}\right) \left(1 - \frac{2\kappa m}{(d-2)\Sigma r^{d-3}}\right)^{-1}, \end{aligned} \quad (\text{B.1})$$

where the metric is as before, i.e. (2.1) with $\Lambda = 0$. They have been studied before in [34] where a higher-dimensional version of Buchdahl's limit was derived. We are interested in the linear and homogeneous equation of state $p = q\rho$ which is the only equation of state that leaves (B.1) invariant under the scale transformation

$$r \rightarrow Cr, \quad \rho \rightarrow C^{-2}\rho, \quad p \rightarrow C^{-2}p, \quad m \rightarrow C^{d-3}m, \quad (\text{B.2})$$

where $C \in \mathbb{R}^+$ [6, 19]. In that case, introducing the dimensionless variables¹³

$$u = \frac{\Sigma r^{d-1} \rho}{m}, \quad v = \frac{\rho}{p} \frac{\kappa m}{(d-2)\Sigma r^{d-3}} \left(1 - \frac{2\kappa m}{(d-2)\Sigma r^{d-3}}\right)^{-1}, \quad (\text{B.3})$$

equations (B.1) are transformed (cf. [19]) to the following autonomous system:

$$\begin{aligned} \frac{du}{d\xi} &= -u(1 - d + u + (d-3 + qu)(1+q)v) \\ \frac{dv}{d\xi} &= -v(d-3-u+2q(d-3-u)v), \end{aligned} \quad (\text{B.4})$$

where $\xi = \ln r$. Note that if m and ρ are positive and the spacetime is static, u and v lie in the ranges $u > 0, v > 0$. In that case, following [19], we change from (u, v) to the bounded variables $(U, V) \in (0, 1)^2$

$$U = \frac{u}{1+u}, \quad V = \frac{v}{1+v}, \quad (\text{B.5})$$

and introduce a new independent variable λ ,

$$\frac{d\lambda}{d\xi} = \frac{1}{(1-U)(1-V)}, \quad (\text{B.6})$$

¹³These may be regarded as a relativistic analogue of the Milne variables, homology invariant variables in the Newtonian theory. If the speed of light c is put back in, we have for a linear equation of state $p = q\rho c^2$, where ρ is now the rest frame mass density. The Newtonian limit is given by $c \rightarrow \infty, q \rightarrow 0$ with qc^2 constant. The Einstein equations then reduce to an Emden equation describing an isothermal sphere in Newtonian gravity [17]. Note that in the Newtonian case a polytropic equation of state also preserves scale invariance [19].

whence equations (B.4) yield the following dynamical system:

$$\begin{aligned}\frac{dU}{d\lambda} &= U(1-U)(d-1-dU-(2d-4+(d-3)q)V+(2d-3+(d-q-4)q)UV) \\ \frac{dV}{d\lambda} &= V(1-V)(1+(2q-1)V)(3-d+(d-2)U).\end{aligned}\quad (\text{B.7})$$

As discussed in [19], the asymptotic properties of a dynamical system are determined by the boundaries, therefore it is essential to consider the compactified state space $[0, 1]^2$. This requires the system to be \mathcal{C}^1 on $[0, 1]^2$, which is clearly the case for the polynomial system (B.7).

The idea is to solve the dynamical system (B.7) for $U(\lambda)$, $V(\lambda)$ on the state space $[0, 1]^2$ and then to obtain the physical perfect fluid configurations $m(r)$, $\rho(r)$ one inverts the transformations (B.3), (B.5), see [19].

A pivotal role in any dynamical systems analysis is played by the fixed points.¹⁴ The fixed points of (B.7) in the unit square $[0, 1]^2$ and their associated eigenvalues are listed in Table 2, where the parameters ω_1 and ω_2 are given by

$$\begin{aligned}\omega_1 &= \frac{(d-3)(1+q)(d-3+(d-1)q)}{2(d-2)(d-1+(d-3)q(2+q))} \\ \omega_2 &= \frac{(d-3)(1+q)\sqrt{(1+q)^2d^2-2(1+q)(7+5q)d+25q^2+22q+33}}{2(d-2)(d-1+(d-3)q(2+q))}.\end{aligned}\quad (\text{B.8})$$

Fixed point	U	V	Eigenvalues
T_1	0	0	$(d-1)$, $-(d-3)$
T_2	$\frac{d-1}{d}$	0	$-\frac{(d-1)}{d}$, $\frac{2}{d}$
T_3	$\frac{d-3}{d-2}$	$\frac{2}{d-1+(d-3)q(2+q)}$	$-\omega_1 \pm \omega_2$
T_4	1	0	1 , 1
T_5	1	1	$q(1+q)$, $-2q$
T_6	0	1	$-(d-3)(1+q)$, $2(d-3)q$

Table 2: Fixed points of (B.7) in the unit square $[0, 1]^2$ and associated eigenvalues, assuming $0 \leq q \leq 1$ and $d \geq 4$.

The global dynamics of the system is determined by its past and future limit sets. For the system (B.7) it takes a particularly simple form: it may be shown (cf. [19]) that orbits in the interior of the unit cube originate either from the fixed point T_2 or from the fixed point T_4 , and converge to the fixed point T_3 .¹⁵ The central role is played by the

¹⁴The Hartman-Grobman theorem states that the eigenvalues and eigenvectors of the linearization of a dynamical system about a hyperbolic fixed point completely characterize the flow of the system in the neighbourhood of this point, that is, the flow of the full non-linear system is topologically equivalent to the flow of its linearization in this neighbourhood.

¹⁵This follows from local analysis and the monotonicity principle, whereby the existence of a monotone function on the state space precludes periodic or recurrent orbits, see [19]. It may be verified that a monotone function is given by $Z = (qh_1 + k_1)^2(uv)^{-p_1}(1 + 2qv)^{p_1-1}$ where $h_1 = (1+q)(d-3+qu)v$, $k_1 = d-3+(d-1)q$ and $p_1 = 4q^2/((1+q)(d-3+(d+1)q))$, cf. [19] for $d = 4$.

fixed point T_2 , corresponding to Minkowski space in spherically symmetric form, and by the fixed point T_3 , which represents the singular self-similar solution (cf. eqn. (2.14))

$$\rho = \alpha r^{-2}, \quad m = \alpha \Sigma r^{d-3}/(d-3) \quad \text{where} \quad \alpha = \frac{2(d-2)(d-3)\kappa^{-1}}{d(d-4)(1+q)^2 + 3q^2 + 6q + 7}. \quad (\text{B.9})$$

Scale invariance implies that the entire set of solutions with a regular centre is represented [19] in the state space by a single orbit originating from T_2 (as $\lambda \rightarrow -\infty$ or $r \rightarrow 0$) and converging to T_3 as (as $\lambda \rightarrow \infty$ or $r \rightarrow \infty$).¹⁶ The exact form of this orbit must be found numerically, however, one may write down asymptotic approximations for it by linearizing the dynamical system about the points T_2 and T_3 : these are determined by the corresponding eigenvalues (and associated eigenvectors) in Table 2. It follows from (B.9) that the regular perfect fluid configurations with $\Lambda = 0$ have infinite mass and are thus not asymptotically flat: to obtain finite mass perfect fluid solutions one must confine the radiation to an unphysical box. Scale invariance then implies that the regular orbit admits a dual interpretation [4], whereby different initial segments (equivalently end points) of the orbit are interpreted as representing distinct regular equilibria of a perfect fluid in a box of fixed radius R , that may be parametrized by their central density ρ_c (a monotonic function of λ), so that T_2 represents the solution with $\rho_c = 0$, i.e. an empty box, and T_3 is the limiting solution as $\rho_c \rightarrow \infty$.

The crucial fact is that the behaviour of the regular orbit as $\lambda \rightarrow \infty$, i.e. in the neighbourhood of the fixed point T_3 , reflects itself in the high-density behaviour of various asymptotic quantities, such as the mass, the red-shifted temperature or the entropy, of a linear (i.e. $p = q\rho$) perfect fluid in a box. Indeed, it was shown in [19] that the equation of state may be quite different away from the centre, as long as it is still asymptotically linear at high densities. They considered a fairly general class of equations of state that are asymptotically linear at high densities and asymptotically polytropic at low densities and proved that the mass-radius diagram of these stellar models has a spiral structure (for low enough polytropic index the radius is finite without the need for a box).¹⁷ The case treated in this paper, where the linear equation of state was modified by adding a negative cosmological constant, giving finite mass unbounded configurations without the need for a box, may be treated similarly.¹⁸

The behaviour of the regular orbit near T_3 is determined by the eigenvalues $-\omega_1 \pm \omega_2$, where ω_1 and ω_2 are given by equation (B.8). These depend on the value of q and on the dimension d . For $0 \leq q \leq 1$ and $4 \leq d < 10$, ω_2 is always imaginary, and the fixed point T_3 is a stable focus (since ω_1 is positive). This leads to oscillatory behaviour, e.g. the spiral structure theorem in [19] or the $4 \leq d \leq 10$ case in this paper. However, for a given $0 \leq q \leq 1$, there is a critical dimension d_{crit} above which ω_2 is real and strictly

¹⁶The one-parameter set of orbits originating from the fixed point T_4 may be continued to the negative mass domain $u < 0$, $v < 0$ and describes solutions with a negative mass singularity surrounded by positive energy density that enter the state space when they have gained enough mass [19].

¹⁷The presence of another, non-scale-invariant, variable in the equations means one has to work with a 3-dimensional dynamical system, i.e. the state space is enlarged to a cube [19]. The key is again scale invariance, which is now only present asymptotically [19].

¹⁸For the case of positive cosmological constant, see [18].

less than ω_1 , i.e. T_3 is a stable node and monotonic behaviour emerges instead. It may be verified that the critical dimension is always in the range $10 \leq d \leq 11$. The case of perfect fluid radiation ($q = 1/(d-1)$) treated in this paper gives a critical dimension $d_{crit} = 10.96404372\dots$. Curiously, a stiff fluid ($q = 1$) gives $d_{crit} = 10$, and pressureless dust ($q = 0$) gives $d_{crit} = 11$. The last result also corresponds to the Newtonian limit (the isothermal sphere) and has been obtained before in [35].

References

- [1] S. W. Hawking and D. N. Page, *Thermodynamics of Black Holes in Anti-de Sitter Space*, *Commun. Math. Phys.* **87** (1983) 577.
- [2] E. Witten, *Anti-de Sitter space, thermal phase transition, and confinement in gauge theories*, *Adv. Theor. Math. Phys.* **2** (1998) 505, [hep-th/9803131](#).
- [3] D. N. Page and K. C. Phillips, *Self-Gravitating Radiation in Anti-de Sitter Space*, *Gen. Rel. Grav.* **17** (1985) 1029.
- [4] R. D. Sorkin, R. M. Wald and Z. Z. Jiu, *Entropy of Self-Gravitating Radiation*, *Gen. Rel. Grav.* **13** (1981) 1127.
- [5] C. B. Collins, *Comments on the static spherically symmetric cosmologies of Ellis, Maartens, and Nel*, *J. Math. Phys.* **24** (1983) 215.
- [6] C. B. Collins, *Static relativistic perfect fluids with spherical, plane, or hyperbolic symmetry*, *J. Math. Phys.* **26** (1985) 2268.
- [7] B. J. Carr and A. A. Coley, *Self-Similarity in General Relativity*, *Class. and Quant. Grav.* **16** (1999) R31, [gr-qc/9806048](#).
- [8] R. Emparan, G. T. Horowitz and R. C. Myers, *Exact description of black holes on branes. II: Comparison with BTZ black holes and black strings*, *JHEP* **0001** (2000) 021, [hep-th/9912135](#).
- [9] R. Emparan, A. Fabbri and N. Kaloper, *Quantum black holes as holograms in AdS braneworlds*, *JHEP* **0208** (2002) 043, [hep-th/0206155](#).
- [10] J. S. Dowker and G. Kennedy, *Finite Temperature And Boundary Effects In Static Space-Times*, *J. Phys. A* **11** (1978) 895.
- [11] K. Kirsten, *Finite Temperature Interacting Scalar Field Theories In Curved Space-Time*, *Class. and Quant. Grav.* **10** (1993) 1461.
- [12] C. P. Burgess, N. R. Constable and R. C. Myers, *The free energy of $N = 4$ Super-Yang-Mills and the AdS/CFT correspondence*, *JHEP* **9908** (1999) 017, [hep-th/9907188](#).
- [13] P. T. Landsberg, A. De Vos, *The Stefan-Boltzmann constant in n -dimensional space*, *J. Phys. A* **22** (1989) 1073.
- [14] C. W. Misner and H. S. Zepolsky, *High-Density Behavior and Dynamical Stability of Neutron Star Models*, *Phys. Rev. Lett.* **12** (1964) 635.
- [15] R. Tooper, *General Relativistic Polytopic Fluid Spheres*, *Astrophys. J.* **140** (1964) 434.
- [16] P. H. Chavanis, *Gravitational instability of finite isothermal spheres*, *Astron. Astrophys.* **381** (2002) 340, [astro-ph/0103159](#).

- [17] P. H. Chavanis, *Gravitational instability of finite isothermal spheres in general relativity. Analogy with neutron stars*, *Astron. Astrophys.* **381** (2002) 709, [astro-ph/0108230](#).
- [18] U. S. Nilsson and C. Uggle, *General Relativistic Stars: Linear Equations of State*, *Ann. Phys. (NY)* **286** (2001) 278, [gr-qc/0002021](#).
- [19] J. M. Heinzle, N. Rohr and C. Uggle, *Spherically Symmetric Relativistic Stellar Structures*, *Class. and Quant. Grav.* **20** (2003) 4567, [gr-qc/0304012](#).
- [20] R. M. Wald, *Entropy and black-hole thermodynamics*, *Phys. Rev. D.* **20** (1979) 1271.
- [21] R. Bartnik, *Existence of maximal hypersurfaces in asymptotically flat spacetimes*, *Commun. Math. Phys.* **94** (1984) 155.
- [22] K. Akutagawa, *Existence of maximal hypersurfaces in an asymptotically anti-de Sitter spacetime satisfying a global barrier condition* *J. Math. Soc. Jap.* **41** (1989) 161.
- [23] A. K. M. Masood-Ul-Alam, *Proof that static stellar models are spherical*, *Gen. Rel. Grav.* **39** (2006) 55.
- [24] I. Papadimitriou and K. Skenderis, *Thermodynamics of asymptotically locally AdS spacetimes*, *JHEP* **0508** (2005) 004, [hep-th/0505190](#).
- [25] A. Karch and L. Randall, *Locally localized gravity*, *JHEP* **0105** (2001) 008, [hep-th/0011156](#).
- [26] N. Kaloper and L. Sorbo, *Locally localized gravity: The inside story*, *JHEP* **0508** (2005) 070, [hep-th/0507191](#).
- [27] O. DeWolfe, D. Z. Freedman and H. Ooguri, *Holography and defect conformal field theories*, *Phys. Rev. D* **66** (2002) 025009, [hep-th/0111135](#).
- [28] I. I. Kogan, S. Mouslopoulos and A. Papazoglou, *A new bigravity model with exclusively positive branes*, [plb5012001140](#), [hep-th/0011141](#).
- [29] S. Thambyahpillai, *A closer look at two AdS(4) branes in an AdS(5) bulk*, *JHEP* **0502** (2005) 034, [hep-th/0409190](#).
- [30] A. Chamblin and A. Karch, *Hawking and Page on the brane*, *Phys. Rev. D* **72** (2005) 066011, [hep-th/0412017](#).
- [31] A. A. Garcia and C. Campuzano, *All Static Circularly Symmetric Perfect Fluid Solutions of 2+1 Gravity*, *Phys. Rev. D* **67** (2003) 064014, [gr-qc/0211014](#).
- [32] S. Deser, R. Jackiw, G. 't Hooft, *Three-dimensional Einstein gravity: Dynamics of flat space*, *Ann. Phys. (NY)* **152** (1984) 220.
- [33] A. Ashtekar and M. Varadarajan, *A striking property of the gravitational Hamiltonian*, *Phys. Rev. D* **50** (1994) 4944, [gr-qc/9406040](#).
- [34] J. Ponce de Leon and N. Cruz, *Hydrostatic equilibrium of a perfect fluid sphere with exterior higher dimensional Schwarzschild spacetime*, *Gen. Rel. Grav.* **32** (2000) 1207, [gr-qc/0207050](#).
- [35] C. Sire and P. H. Chavanis, *Thermodynamics and collapse of self-gravitating Brownian particles in D dimensions*, *Phys. Rev. E* **66** (2002) 046133, [cond-mat/0204303](#).
- [36] V. A. Belinsky, I. M. Khalatnikov and E. M. Lifshitz, *Oscillatory approach to a singular point in the relativistic cosmology*, *Adv. Phys.* **19** (1970) 525.

- [37] J. Demaret, M. Henneaux and P. Spindel, *Nonoscillatory Behavior In Vacuum Kaluza-Klein Cosmologies*, *Phys. Lett. B* **164** (1985) 27.
- [38] Y. Elskens and M. Henneaux, *Chaos in Kaluza-Klein Models*, *Class. and Quant. Grav.* **4** (1987) L161.
- [39] V. E. Hubeny, H. Liu and M. Rangamani, *Bulk-cone singularities and signatures of horizon formation in AdS/CFT*, *JHEP* **0701** (2007) 009, [hep-th/0610041](#).
- [40] J. Hammersley, *A critical dimension for the stability of radiating perfect fluid stars*, [arXiv:0707.0961](#).
- [41] P. H. Chavanis, *Relativistic stars with a linear equation of state: analogy with classical isothermal spheres and black holes*, [arXiv:0707.2292](#).